High-Q Factor Multiferroic Resonant MEMS Low Frequency Magnetic Field Sensors

Michael D'Agati, Sydney Sofronici, Yujia Huo, Roy H. Olsson III
University of Pennsylvania
Philadelphia, USA

Peter Finkel, Konrad Bussmann
Thomas Mion, Margo Staruch
Naval Research Laboratory
Washington, D.C., USA

Keith McLaughlin, Brad Wheeler
Leidos
Arlington, USA

***Summary*—Multiferroic resonant MEMS magnetometers show great promise to provide a highly sensitive, low noise option for detecting low frequency magnetic fields at room temperature and in a small form factor. Strain modulation techniques enable sensitivity enhancement by the high device Q factors. However, as the strain modulation increases, a resonator Duffing nonlinearity is observed before the magnetostrictive material can be sufficiently strained to provide high modulation efficiency. Here, we report a multiferroic resonant MEMS magnetometer with a sensitivity of 32mA$_{rms}$/T and noise value of ~2.2nT/√Hz.**

Keywords—MEMS; Multiferroics; Magnetometers; Magnetic Sensing; Aluminum Nitride; Iron Cobalt; Modulation

I. Introduction

MEMS magnetic field sensors have been increasingly sought after for consumer electronics, space research [1], and biomedical applications due to their small volume, high sensitivity, and low noise. Detecting small magnetic fields over a large bandwidth (>1kHz) with low noise remains challenging. Current magnetometers can meet the required sensitivity and noise levels needed to sense magnetic fields produced by the body, but their size and power consumption are too large to be practical for this application. As shown in Fig. 1, this study sets out to create a bio-magnetic sensor with high sensitivity and low noise that is small and consumes little power.

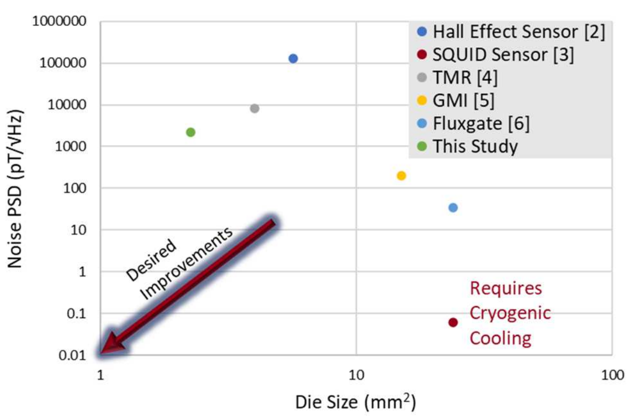

Fig. 1: Comparison of different magnetic sensor technologies' size and magnetic noise value.

Previous multiferroic sensors have utilized a modulation technique, whereby the lower frequency magnetic fields to be sensed are mixed to a higher frequency of operation via strain modulation of a magnetostrictive material [7,8]. Modulation of the signal into the mechanical resonance band of the sensor provides an enhancement in the response proportional to the Q factor of the MEMS component, which can be >1000. When the mechanical resonance is at a high frequency, wide bandwidth, high sensitivity, and low noise can be simultaneously achieved. Here, we report a resonant MEMS multiferroic magnetic field sensor that resonates in a plate extensional mode at 7.8 MHz. The device utilizes aluminum nitride (AlN) as the piezoelectric material, an iron cobalt (FeCo)-based magnetostrictive material, and occupies a die area of 2.25mm^2. By driving the sensor with a modulation amplitude just below the duffing nonlinearity, a sensitivity of 32mA$_{rms}$/T and noise value of ~2.2nT/ √ Hz is achieved.

II. Device Structure and Microfabrication

The plates were designed for a resonance frequency of ~8MHz in the extensional mode. Using (1), originally presented in [9] where v is the wave velocity, E_{eq} is the equivalent Young's modulus, ρ_{eq} is the equivalent density, and t_i is the thickness of each layer, devices were designed with a length of 400um and a width of 100um, with a 1µm thick AlN layer and 0.5µm thick FeCo layer, a 150nm thick Pt bottom electrode, and a 200nm thick Al top electrode, as shown in Fig. 2.

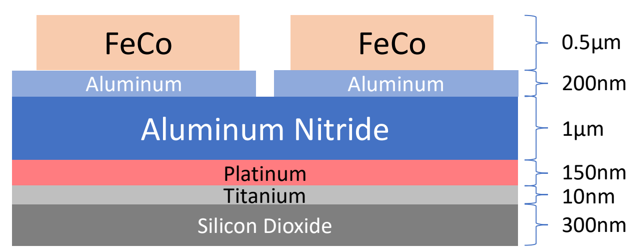

Fig. 2: Cross-section layer stack of multiferroic resonator.

$$v = \sqrt{\frac{E_{eq}}{\rho_{eq}}} = \sqrt{\frac{\Sigma(t_i * E_i)}{\Sigma(t_i * \rho_i)}} \quad (1)$$

When an alternating magnetic field is present along the longitudinal direction, the FeCo strains, causing the mechanically coupled AlN to expand and contract, generating a time varying electrical output signal. Simultaneously, a time varying stress excitation is applied to the magnetostrictive material by applying a modulation voltage to the piezoelectric layer via the drive electrode shown in Fig. 3. Doing so causes

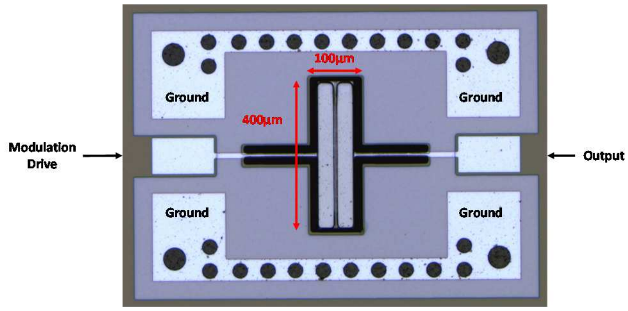

Fig. 3: Top-down optical image of a multiferroic resonator device.

the magnetostrictive curve of the FeCo to shift similarly to that shown in Fig. 4. As the magnetostrictive curve shifts in response to a change in stress, the point of maximum strain per magnetic field (d_{33}) changes. Maximizing this change in piezomagnetic coefficient (Δd_{33}) is the key to obtaining a highly sensitive multiferroic magnetic sensor mixed up at higher frequencies. The mixed signal, in response to magnetic field, is collected by the output electrode.

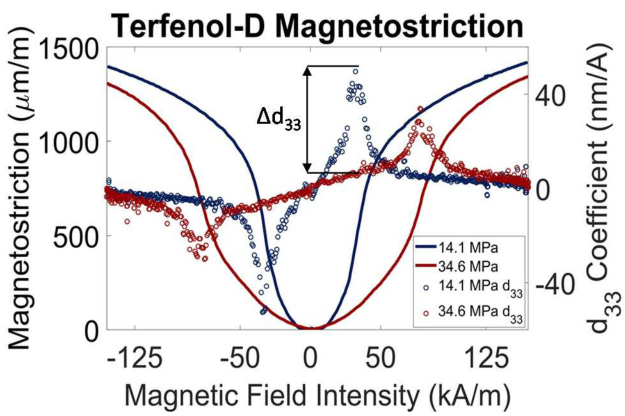

Fig. 4: Modified magnetostrictive curve of Terfenol-D showing a change in the d_{33} coefficient with a change in stress applied. [10]

Four photomasks were used to fabricate the magnetometers. Wafers were purchased from MTI Corporation with 300nm SiO_2, 10nm Ti, and 150nm Pt (111) deposited on low resistivity 100mm diameter Si wafers. The Ti/Pt films were patterned by wet etching in Aqua Regia to form the bottom electrodes. Next, 1μm of AlN was sputtered using an Evatec Clusterline© 200 system, producing films with a rocking curve full width half maximum (FWHM) of <2° and a surface roughness less than 3nm. Vias to the Pt bottom electrodes were patterned by wet etching in 30% KOH. 200nm thick Al top electrodes were sputtered and patterned by dry etching in an Oxford Cobra ICP system. The Al ground top electrodes were connected down to the Pt bottom layer through the vias, taking advantage of the sloped sidewall created by the KOH wet etch. Next, chlorine dry etching was performed to etch the AlN at the perimeter of the device, aligned with the Pt that was previously etched away in that location. Doing so defines the dimensions of the device and opens a region down to the Si beneath. A bi-layer liftoff step was used for patterning a 500nm thick FeCo-based magnetostrictive material deposited by magnetron sputtering at the Naval Research Laboratory (NRL). Lastly, XeF_2 was used to release and suspend the resonant plates by attacking the Si exposed to the surface in the earlier step.

III. CHARACTERIZATION

The sensor in Fig. 3 was first electrically characterized via an S_{21} measurement using a Keysight P9372A vector network analyzer (VNA) to measure the plate's natural mechanical resonance frequency and quality factor. Also measured on the VNA was the modulation voltage amplitude that results in Duffing nonlinearity. Increasing the modulation voltage provides a higher modulated output signal, or higher sensitivity, in response to magnetic field. When the Duffing nonlinearity presents itself though, the noise floor rapidly increases, leading to a degradation in signal-to-noise ratio (SNR) with increasing modulation amplitude. Magnetic testing was performed using the setup shown in Fig. 5. A Keysight 3600A series signal generator was used to drive the piezoelectric layer at its resonance frequency with a voltage under the mechanical

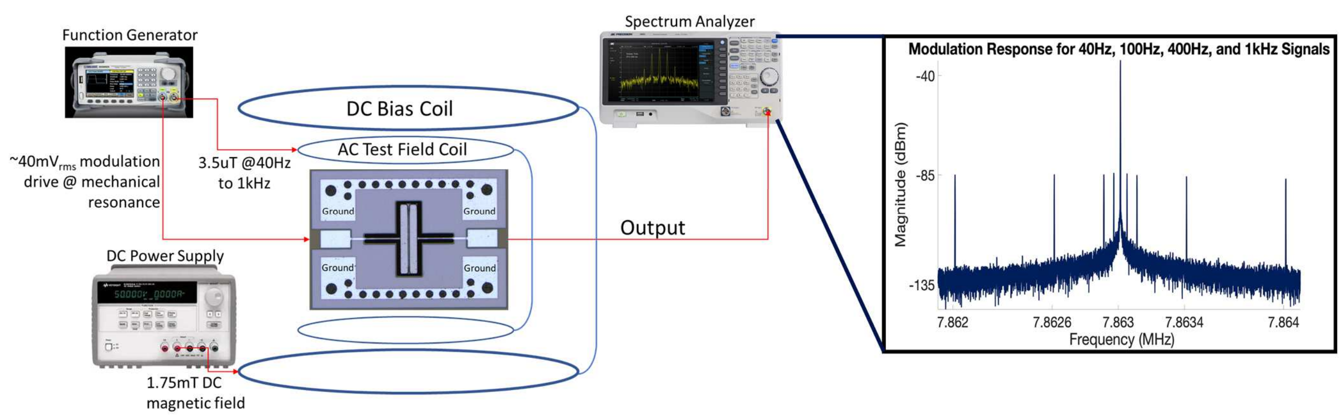

Fig. 5: Modulation testing setup providing AC magnetic sensing fields, modulation voltage signal, and a DC magnetic bias field along with an example modulation response collected at the output on a spectrum analyzer. This example response has 4 different measurements, at 40,100, 400 and 1000 Hz, superimposed on one graph.

nonlinearity regime determined by the VNA. RF coils were also driven by the signal generator at a frequency between 1Hz and 1kHz, simulating the frequency of biological magnetic signals. A DC power supply provided a DC magnetic bias field of 1.75mT to the magnetostrictive material through an electromagnet. The output of the device is collected by a Rigol RSA3045 spectrum analyzer. Demodulation of the output signal was performed using switches prior to digitizing the output with a National Instruments DAC card.

IV. Discussion and Conclusion

Figure 6 shows the S_{21} response of the sensor demonstrating a resonance frequency of 7.83MHz and a loaded Q factor of 1779 in ambient pressure conditions. The high Q factor of this

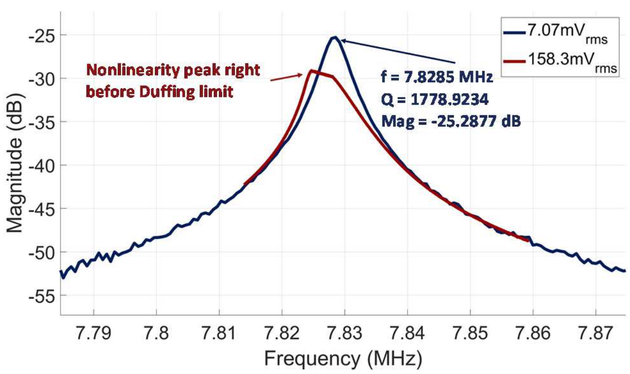

Fig. 6: S_{21} plots showing the resonance peak at 7mV$_{rms}$ and 158mV$_{rms}$ applied voltages. At a high enough voltage, Duffing nonlinearity is observed.

device results in significant enhancement of the output signal when modulated at mechanical resonance. Providing a small AC magnetic field of 3.5uT$_{rms}$ directly at the mechanical resonance frequency gives a large sensitivity value close to 1A/T and a sensor resolution ~ 20 pT/ √ Hz, which is limited by the ~20 pA/ √ Hz noise floor of the readout electronics. The output signal shown in Fig. 5 demonstrates a modulated sensor response of 67mA/T with an 80mV$_{rms}$ modulation applied. Constant sensitivity is observed for a 3.5uT$_{rms}$ input magnetic field at 40, 100, 400, and 1000 Hz. With ideal modulation, the modulated sensitivity and SNR should approach that of direct RF excitation at resonance. When modulating the device close to the Duffing limit, sensitivities in excess of 100mA/T have been realized, but

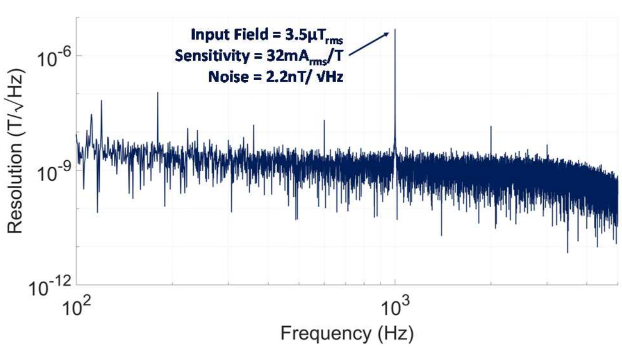

Fig. 7: Demodulated output signal showing the desired signal peak at 1kHz with a noise value of 2.2nT/√Hz.

with degraded SNR. This result indicates that it will be critical to identify methods to sufficiently strain modulate the magnetic material before inducing resonator Duffing nonlinearity to achieve the desired noise characteristics from multiferroic sensors. When driving the modulation voltage at 40mV$_{rms}$, far enough below 158mV$_{rms}$ to ensure no degradation in the SNR due to nonlinearity, a sensitivity of 32mA/T and a demodulated resolution of approximately 2.2nT/ √ Hz are achieved over a bandwidth of 100 Hz to 1 kHz. The sensitivity and noise resolution values are obtained from the demodulated signal presented in Fig. 7. Future research will seek to optimize the design and materials to increase the strain modulation of the magnetostrictive material prior to reaching the duffing limit. Future studies will also attempt to increase the Q factor through vacuum packaging and decrease the noise of the system through improvements to the readout circuitry.

Acknowledgment

This work was partially supported by the DARPA QUIVER program under grant number HR0011-20-C-0098. This material is based upon work supported by the National Science Foundation Graduate Research Fellowship under grant award number DGE-1845298. This work was carried out in part at the Singh Center for Nanotechnology, which is supported by the NSF National Nanotechnology Coordinated Infrastructure Program under grant NNCI-2025608.

References

[1] Séran, H. C., and P. Fergeau. "An optimized low-frequency three-axis search coil magnetometer for space research." Review of scientific instruments 76.4 (2005): 044502.

[2] Allegro Microsystems Inc. AAllegro A1324, A1325, and A1326 Low Noise, Linear Hall Effect Sensor ICs with Analog Output 2010-2011.

[3] Granata, C., A. Vettoliere, and M. Russo. "An ultralow noise current amplifier based on superconducting quantum interference device for high sensitivity applications." Review of Scientific Instruments 82.1 (2011): 013901.

[4] Mazumdar, Dipanjan, et al. "Thermal stability, sensitivity, and noise characteristics of MgO-based magnetic tunnel junctions." Journal of applied physics 101.9 (2007): 09B502.

[5] Aichi Steel Corporation Nano Tesla Sensor MI-CB-1DH [Available from: (https://aichi-mi.com/app/download/10290224492/Leaflet+MI-CB-1DH.pdf?t=1420787919).

[6] Vértesy, Gábor, Antal Gasparics, and J. Szöllősy. "High sensitivity magnetic field sensor." Sensors and Actuators A: physical 85.1-3 (2000): 202-208.

[7] Zaeimbashi, Mohsen, et al. "Ultra-compact dual-band smart NEMS magnetoelectric antennas for simultaneous wireless energy harvesting and magnetic field sensing." Nature communications 12.1 (2021): 1-11.

[8] Hayes, P., et al. "Electrically modulated magnetoelectric sensors." Applied Physics Letters 108.18 (2016): 182902.

[9] Kim, Bongsang, Roy H. Olsson, and Ken E. Wojciechowski. "AlN microresonator-based filters with multiple bandwidths at low intermediate frequencies." Journal of microelectromechanical systems 22.4 (2013): 949-961.

[10] Tdvib.com. 2022. [online] Available at: <http://www.tdvib.com/wp-content/uploads/2015/09/Terfenol-D-Magnetostriction.png> [Accessed 31 March 2022].